

1 **DNA extraction and virome processing methods strongly**  
2 **influence recovered human gut viral community characteristics**

3 *Short title –Processing Method Shapes Gut Virome Data*

4 Luke S. Hillary<sup>1</sup>, Trina A. Knotts<sup>2,3,4</sup>, Sean H. Adams<sup>2,3,4</sup>, Mohamed R. Ali<sup>2,3,4</sup>, Matthew R. Olm<sup>5</sup>, Joanne  
5 B. Emerson<sup>1\*</sup>

6 1 - Department of Plant Pathology, University of California, Davis, USA

7 2 - Department of Surgery, University of California, Davis School of Medicine, Sacramento, USA

8 3 – Center for Alimentary and Metabolic Science, University of California Davis School of Medicine,  
9 Sacramento, California, USA

10 4 –Nutrition for Transformative Healthcare Program, University of California Davis School of Medicine,  
11 Sacramento, USA

12 5 – Department of Integrative Physiology, University of Colorado, Boulder, USA

13 Contact details:

14 \*Corresponding author

15 [jbemerson@ucdavis.edu](mailto:jbemerson@ucdavis.edu)

16 Department of Plant Pathology, Hutchison Hall, 425 Storer Mall, University of California, Davis CA,  
17 95616, USA

## *Processing Method Shapes Gut Virome Data*

### 18 **Abstract**

19 Accurately characterising the human gut virome is critical to understanding virus-microbiome-host  
20 interactions. However, widely used methods introduce biases that complicate data interpretation and limit  
21 cross-study comparability. For instance, multiple-displacement amplification (MDA) preferentially  
22 amplifies single-stranded DNA viruses, while total metagenomes are dominated by non-viral sequences,  
23 reducing viral signal. These traditional methods have not been systematically compared to viral size-  
24 fraction metagenomes (viromes) prepared without MDA. To address this, we applied four common  
25 methods for characterising human gut viral community composition (total metagenomes, viromes with/  
26 without DNase treatment (to remove free DNA), and MDA viromes) to a human stool sample, with  
27 technical triplicates for each approach. MDA biased viral community composition to a shocking degree:  
28 *Microviridae* formed ~90% of MDA viromes compared to just 2% of non-MDA viromes. Removing  
29 ssDNA viruses from data analyses substantially reduced, but did not eliminate, MDA bias. Metagenomes  
30 were enriched for putative temperate phages and predicted *Bacillota-phages*, whereas predicted  
31 *Bacteroidetes*-phages dominated all viromes, suggesting that metagenomes and viromes select for  
32 different populations within the total viral community. DNase treatment had little-to-no effect on virome  
33 richness or community composition. This proof-of-principle experiment demonstrates that preparatory  
34 methods for viral community analysis can lead to substantially different conclusions from the same faecal  
35 sample, and we provide a comprehensive omic data analysis framework for comparing laboratory  
36 methodologies for viral ecology. With sufficient DNA yields now easily achievable from human gut  
37 viromes without the use of MDA, our results suggest that this biased amplification method should be  
38 avoided in human gut virome studies.

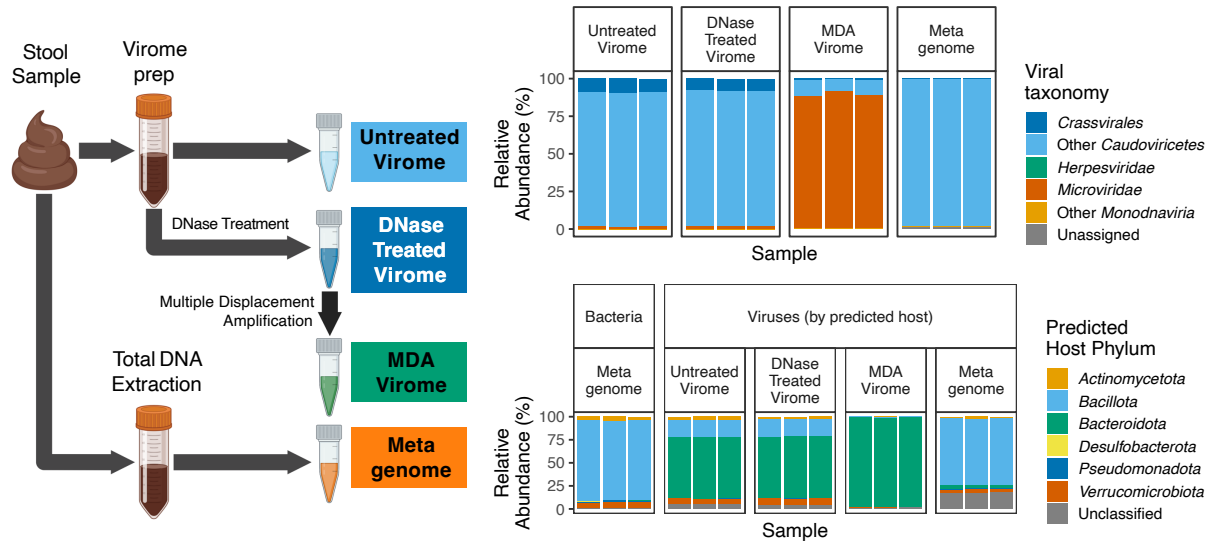
### 39 **Keywords**

40 Human gut virome, metagenomics, viral ecology, multiple displacement amplification, DNase treatment,  
41 virus-host interactions, sequencing methods

## Processing Method Shapes Gut Virome Data

### 42 Graphical Abstract

# DNA extraction and virome processing methods strongly influence recovered human gut viral community characteristics



## *Processing Method Shapes Gut Virome Data*

### 53 **Introduction**

54       The viruses present in the human gastrointestinal tract, otherwise known as the gut virome, have the  
55 potential to regulate the composition, activity, and functional capacity of the gut microbiome through cell  
56 lysis, altered cellular metabolism, and horizontal gene transfer (1,2). Viral dysbiosis, a disruptive  
57 imbalance of the human gut virome (e.g. lower diversity), is associated with various disease states and  
58 may act as a diagnostic indicator in inflammatory bowel disease and pancreatic cancer (3–6). Phage  
59 therapy, via individual phages, phage cocktails, and whole-virome transplants, has the potential to address  
60 issues related to antimicrobial resistance and targeted interventions in gastrointestinal diseases (7,8).  
61 Therefore, accurate characterisation of the gut virome composition and dynamics is of critical importance.

62       Human gut virome studies often use either faecal shotgun metagenomics or size-selective viromics to  
63 characterise viral community composition, functional capacity, and ecological dynamics (9–11).  
64 Comparative studies in soils and aquatic environments show that while total metagenomes capture  
65 integrated prophages, giant viruses excluded by size-selection, and actively-replicating viruses often  
66 absent from the viral size fraction, they can recover less fine-scale diversity than size-selective viromes  
67 (12–14). Thus, metagenomics and viromics can differ in recovered viral community compositions (15),  
68 but systematic comparisons across different techniques remain limited.

69       Previous work on improving viral community characterization has focused on optimizing sample  
70 handling (16), viral concentration methods (17,18), nucleic acid extraction (19,20), PCR amplification  
71 cycles (21), and sequencing library preparation (22). As many of these studies focused on mock  
72 communities or viral spike-ins, viral recovery and diversity metrics were the primary evaluation criteria.  
73 This leaves clear knowledge gaps in how different methods affect recoverable virome diversity within  
74 complex human gut communities.

75       The amount of faecal material available for DNA extraction can be limited, leading to an assumed  
76 need for amplification to achieve sufficient yields for sequencing. This is often accomplished via high

## *Processing Method Shapes Gut Virome Data*

77 numbers of PCR cycles (>6-8) during sequencing library preparation or through an initial treatment of  
78 multiple displacement amplification (MDA) before library construction (21,23). However, MDA is  
79 known to bias viromes towards amplifying small circular DNA, leading to the presumed but rarely  
80 quantified overrepresentation of single-stranded DNA viruses, such as *Microviridae*, in MDA-viromes  
81 from diverse environments (24,25). Given this known bias, systematic tests comparing viral communities  
82 recovered from MDA viromes and non-MDA viromes are needed.

83 Although the effects of DNase treatment have not been systematically evaluated for human gut  
84 viromes, studies in soil show that freezing can lead to viromic DNA yields below detection limits after  
85 DNase treatment (26,27), presumably because freezing compromises virions and exposes viral genomic  
86 DNA to enzymatic degradation. In agricultural soils, DNase treatment on fresh samples resulted in a 53%  
87 reduction in viral diversity, although broader community structure and ecological patterns remained  
88 similar with and without DNase treatment (28). As most faecal samples from human studies are stored  
89 frozen for logistical reasons, and storage above freezing has been shown to alter microbial community  
90 composition (29), the effects of DNase treatment on previously-stored faecal viromes warrant further  
91 consideration. Given that omitting DNase treatment improves viral recovery from frozen soil samples, the  
92 potential for skipping DNase treatment on faecal samples stored frozen should be evaluated, especially  
93 since low DNA yields might make biased MDA more tempting.

94 Here we leveraged our soil viromics protocol (largely similar to existing protocols in the human gut  
95 literature - Conceição-Neto et al., 2015; Kleiner et al., 2015; Wang et al., 2023) to: (i) compare two types  
96 of virome preparations (with and without DNase treatment – Sorensen et al., 2021), (ii) add a multiple-  
97 displacement amplification (MDA) treatment to aliquots from the DNase-treated viromes, an approach  
98 commonly applied in the human gut virome literature (31), and (iii) compare all of the virome  
99 preparations to “total metagenomes,” commonly used for viral community recovery from a variety of  
100 ecosystems, including soil and the human gut (32,33). With analyses considering percent viral reads, viral  
101 contigs assembled *de novo* vs. recoverable through read mapping to a reference set, viral genome quality,

## *Processing Method Shapes Gut Virome Data*

102 viral richness, viral community beta-diversity, viral taxonomy, predicted host taxonomy, predicted viral  
103 replication strategies, library k-mer complexity, functional annotations, viral genome coverage depth to  
104 enable strain-level analyses, and comparisons to a comprehensive gut viral genomic database, we also  
105 provide an example for rigorous comparisons of the downstream omic data resulting from methodological  
106 differences. Since the faecal material here was stored frozen (experiencing a single freeze-thaw), we  
107 hypothesised that DNase treatment would yield insufficient DNA for sequencing without further  
108 amplification and that viromes without DNase treatment would recover the highest viral diversity. We  
109 hypothesised that these viromes would recover vastly more viral species than total metagenomes and that  
110 MDA viromes would preferentially recover *Microviridae* (small, single-stranded circular DNA viruses),  
111 rendering MDA viromes non-quantitative and not representative of the non-MDA viral community. To  
112 test these hypotheses and provide guidance for future studies, we systematically compared untreated,  
113 DNase-treated, and MDA viromes against metagenomes from the same single faecal source material. This  
114 design allowed us to directly assess how upstream processing choices shape downstream characterisation  
115 of the gut virome, providing an observational benchmark to inform future experimental design.

## 116 **Materials and methods**

### 117 **Sample collection and study design**

118 Faecal sub-samples were generated from a single stool sample collected from a healthy female  
119 participant recruited from the UC Davis bariatric surgery clinic during the pre-operative period, and while  
120 consuming a typical diet. The participant provided informed consent, sample collection protocols were  
121 approved by the UC Davis Institutional Review Board, and the studies conform to the Declaration of  
122 Helsinki (34). The stool material was stored intact at -80 °C until processing. A 100 g stool sample was  
123 thawed overnight at 4°C and manually homogenised, followed by sub-sampling for DNA extraction.

## *Processing Method Shapes Gut Virome Data*

124 In total, four approaches to measure viral community composition were compared in triplicate (see  
125 Supplementary Fig. S1): untreated viromes, DNase-treated viromes, MDA viromes (DNase-treated  
126 viromic DNA that was subsequently treated with multiple-displacement amplification, MDA), and stool  
127 total metagenomes.

### 128 **Virome sample processing**

129 For viromes, virus-like particles (VLPs) were purified from six 10 g sub-samples of thawed stool as  
130 previously described for soil (35). Briefly, VLPs were purified from stool by three sequential rounds of  
131 suspension in 9 mL of protein-supplemented PBS buffer (PPBS - 2% bovine serum albumin, 10%  
132 phosphate-buffered saline, 150 mM MgSO<sub>4</sub>) in 50 mL conical tubes, each followed by 10 minutes of  
133 orbital shaking at 300 rpm, 4°C, and 10 minutes centrifugation at 4,000 × g, 4 °C. Supernatants from the  
134 first and second rounds were stored in separate 50 mL conical tubes at 4 °C during subsequent rounds of  
135 resuspension, shaking, and centrifugation. Supernatants from each aliquot were combined, centrifuged at  
136 10,000 × g at 4°C for 8 minutes, and the supernatant was retained, followed by a second round of  
137 centrifugation. Supernatants were filtered sequentially through 5 μm, 0.45 μm, and 0.2 μm PES  
138 (polyethersulfone) syringe filters and pooled in 50 mL conical tubes prior to being transferred to 26.3 mL  
139 polycarbonate round-bottomed ultracentrifuge tubes (Beckman-Coulter Life Sciences), followed by  
140 ultracentrifugation at 35,000 rpm (112,000 × g) at 4 °C for 145 minutes using an Optima LE-80K  
141 ultracentrifuge and 50.2 Ti rotor (Beckman-Coulter Life Sciences). Supernatants were discarded, and  
142 pellets resuspended in 600 μL nuclease-free water. DNase treatment was performed on three 100 μL  
143 aliquots of VLP concentrate by incubating them with 10 μL RQ1 DNase and 10 μL RQ1 DNase buffer  
144 (Promega) for 30 minutes at 37 °C. DNase was inactivated by the addition of 10 μL of RQ1 DNase stop  
145 solution (Promega).

146

## *Processing Method Shapes Gut Virome Data*

### 147 **Virome and metagenome DNA extraction, multiple-displacement** 148 **amplification, and library construction**

149 DNA was extracted from 100  $\mu$ L aliquots of VLP concentrates (untreated viromes), the DNase-  
150 treated virome preparations, or 0.25 mg of stool (for metagenomes), using the PowerSoil Pro DNA  
151 extraction kit (Qiagen) per manufacturer's instructions. Samples were incubated with lysis buffer for 10  
152 minutes at 65 °C followed by vortexing for 10 minutes at maximum speed. Further steps were carried out  
153 according to the manufacturer's instructions. DNA was quantified using a Qubit 1x High Sensitivity DNA  
154 quantification assay and Qubit 4 fluorimeter (Thermo Fisher Scientific, Inc.).

155 To generate the MDA viromes, three 1  $\mu$ L aliquots of DNA from each of the three DNase-treated  
156 virome preparations were used as templates for MDA, for nine reactions in total. MDA was performed  
157 using the GenomiPhi V2 DNA amplification kit (Cytiva), according to the manufacturer's instructions.  
158 The nine reactions were then pooled into three treatment replicates (three MDA reactions per DNase-  
159 treated virome), yielding three MDA virome preparations.

160 Libraries for all four methods (3 $\times$  untreated viromes, 3 $\times$  DNase-treated viromes, 3 $\times$  MDA viromes,  
161 3 $\times$  metagenomes) were prepared using the KAPA DNA HyperPrep library kit (Roche) by the DNA  
162 Technologies & Expression Analysis Core, UC Davis, and 150 bp paired-end sequencing was performed  
163 to a target depth of 20 Gbp per library using the Illumina NovaSeq 6000 platform.

### 164 **Sequencing data quality control**

165 Detailed data processing settings are provided in Supplementary Table S2. Raw reads were trimmed  
166 and filtered using BBDuk v39.1, error-corrected using Tadpole, and deduplicated using Clumpify (all part  
167 of BBTools v39.1 Bushnell 2018). Raw and processed read quality was assessed using FastQC v0.12.1  
168 (Andrews 2010) and MultiQC v1.14 (Ewels et al. 2016).

169

## *Processing Method Shapes Gut Virome Data*

### 170 **Library complexity, rRNA gene read, and human read analyses**

171 K-mer (k=31) frequencies were calculated using khmer v2.1.1 (36). Ribosomal RNA gene reads were  
172 identified using SortMeRNA v4.3.6 (37). Taxonomic profiling of raw reads was performed using  
173 SingleM v0.18.3 (38). To identify human host reads, error-corrected reads were mapped to the human  
174 genome (GCF\_009914755.1, Nurk et al., 2022) using Minimap2 v2.26 (40) and Samtools v1.17 (41).  
175 Count data were aggregated using CoverM v0.6.1 (42).

### 176 **Assembly and viral contig identification**

177 Reads from each library were separately assembled (12 assemblies) using MEGAHIT v1.2.9 (43),  
178 and summary statistics were produced using Quast v5.2.0 (44). Viral contigs were identified from each  
179 assembly using geNomad v1.7.0 (45) and additionally filtered by length  $\geq 10$  Kbp (46) or with a  
180 requirement for both a length between 1 and 10 Kbp and a geNomad phylum = *Monodnaviria*. The latter  
181 requirement facilitates inclusion of single-stranded DNA viruses that typically possess genomes  $< 10$  Kbp  
182 (47).

### 183 **vOTU clustering, read mapping, and community compositional analyses**

184 All viral contigs were clustered together into vOTUs, using a combination of MegaBLAST v2.14.0  
185 and custom Python scripts (see Data and Code Availability), requiring a minimum average nucleotide  
186 identity (ANI) of 95% across 85% of the length of the shortest contig (48–50). Quality-filtered and error-  
187 corrected reads from each library were mapped to dereplicated vOTUs using minimap2 (40) and relative  
188 abundances calculated using transcripts per million (TPM) values generated by CoverM v0.6.1 (42).

189 The presence of vOTUs in a sample was determined using two complementary criteria: detection by  
190 read mapping and recovery of viral contigs through a combination of mapping and assembly. For vOTUs  
191 categorised as “mapped” a vOTU was considered shared between two libraries if  $\geq 75\%$  of its length was  
192 covered at  $\geq 1x$  read depth and 90% ANI in both libraries. vOTUs were considered “assembled” in a

## *Processing Method Shapes Gut Virome Data*

193 library if, in addition to reads mapping to the vOTU sequence according to the aforementioned thresholds,  
194 a viral contig from the same vOTU cluster was assembled from that same library.

195 To identify known vOTUs from the Unified Human Gut Virome catalogue (UHGV,  
196 <https://github.com/snayfach/UHGV>, accessed on June 12<sup>th</sup> 2025) (31,49,51–60) within libraries from this  
197 study, all UHGV vOTUs >10Kbp in length or >50% complete were downloaded from  
198 <https://portal.nersc.gov/UHGV/> on June 12<sup>th</sup> 2025. These UHGV vOTUs were clustered with all 2,480  
199 predicted viral contigs from this study using the same parameters as above, and reads from our libraries  
200 were mapped to this dereplicated set. A UHGV vOTU was considered detected in our dataset if it  
201 clustered with at least one viral sequence from this study or if read mapping covered the vOTU in at least  
202 one sample at the same detection thresholds described above.

### **203 Read depth analysis**

204 Raw reads were randomly sub-sampled to depths of 1 Gbp increments from 1-17 Gbp using seqtk  
205 v1.4-r122 (<https://github.com/lh3/seqtk>), and quality control, assembly, viral contig identification, vOTU  
206 clustering, and read mapping were performed on each subsampled dataset as described above.

### **207 Viral translated protein annotation**

208 As the gene content of vOTU cluster sequences can differ from the vOTU representative sequence, all  
209 viral translated proteins from predicted viral contigs by geNomad were annotated in bulk using Pharokka  
210 v1.7.1 with database v1.4.0 (61).

### **211 vOTU lifestyle and host predictions**

212 Viral lifestyle, i.e., whether a virus is virulent or temperate, was predicted using BACPHLIP v0.9.6  
213 (62). vOTUs were classified as putatively virulent or temperate if the confidence score for either  
214 assignment was  $\geq 0.95$ ; otherwise, they were labelled unclassified. vOTU host prediction was performed  
215 using iPHoP v1.3.2, with a combined prediction confidence score to genus level of  $\geq 90/100$  (63). When

## *Processing Method Shapes Gut Virome Data*

216 two hosts were predicted, the host with higher confidence was selected. If confidence scores were equal,  
217 host prediction was converted to the lowest common taxonomic level.

### **Data analysis and visualization**

219 Statistical analyses and data visualization were performed using R v4.4.0, RStudio v2024.09.1-394,  
220 ggpubr (64), and tidyverse (65). Statistically significant differences with p-values <0.05 were identified  
221 using analysis of variance (ANOVA) and post-hoc Tukey tests and converted into compact letter displays  
222 using multcompView (66). Venn diagrams were visualised using ggVennDiagram (67). Principal  
223 Coordinates Analyses (PCoA) of pairwise Bray-Curtis dissimilarity matrices were performed using  
224 Vegan (68), and significant differences were identified by permutational multivariate analysis of variance  
225 (PERMANOVA).

### **Results and discussion**

#### **Recovered viral communities differed across all processing methods, except between DNase-treated and untreated viromes**

229 To evaluate the impacts of total metagenomics, virus-like particle (VLP) fractionation (viromics),  
230 DNase treatment, and multiple displacement amplification (MDA) on recoverable faecal viral community  
231 composition (Supplementary Fig. S1a), 12 libraries were generated from one stool sample, sequenced to  
232 an average depth of  $21.1 \pm 2.3$  Gbp, and analysed. A total of 2,480 viral contig sequences were identified  
233 using geNomad (45) and clustered into 605 viral operational taxonomic units (vOTUs; Supplementary  
234 Fig. S2). Full results of statistical tests (ANOVA and Tukey post hoc comparisons) for all analyses are  
235 provided in Supplementary Tables S5–S6.

236 Because all preparations were performed on aliquots of the same faecal sample, observed differences  
237 reflect the influence of processing method rather than inter-individual variation, which is a known major

## *Processing Method Shapes Gut Virome Data*

238 source of variability in gut virome studies (2). While this single-sample design limits generalisability, it  
239 provides a clear view of methodological biases in isolation, supporting observational conclusions about  
240 their effects on detectable viral community composition and downstream analyses typically employed in  
241 intervention-based human gut virome studies.

242 The similarity between DNase-treated and untreated viromes following frozen stool sample storage  
243 was unexpected, as DNase treatment is often discouraged for environmental samples stored frozen since it  
244 can result in a 10- to 100-fold loss in viromic DNA yield (69). The negligible impact observed here likely  
245 reflects stool-specific factors, such as (i) higher viral loads and organic content, supporting higher intact  
246 viral particle recovery (15) and/or new virus production during thawing or (ii) a naturally high ratio of  
247 encapsidated to free DNA due to DNase I secretion in the small intestine (70). Unlike soils, where freeze-  
248 thaw cycles may damage a greater proportion of viral capsids (potentially due to higher viral diversity and  
249 overall lower biomass), stool VLP concentrates appear to retain sufficient encapsidated viral DNA to  
250 permit effective sequencing of frozen samples, even after DNase treatment. Together, these findings are  
251 particularly relevant to studies using frozen, biobanked, or transported samples without guaranteed cold-  
252 chain preservation above 0 °C. Of course, further tests using additional samples and comparisons between  
253 fresh and frozen stool samples would be required to assess the generalizability of these results. As DNase-  
254 treated and untreated viromes were virtually indistinguishable in each of our analyses in this study, we  
255 generally describe their results together and refer to them collectively as non-MDA viromes, but we retain  
256 them separately in calculations and figures.

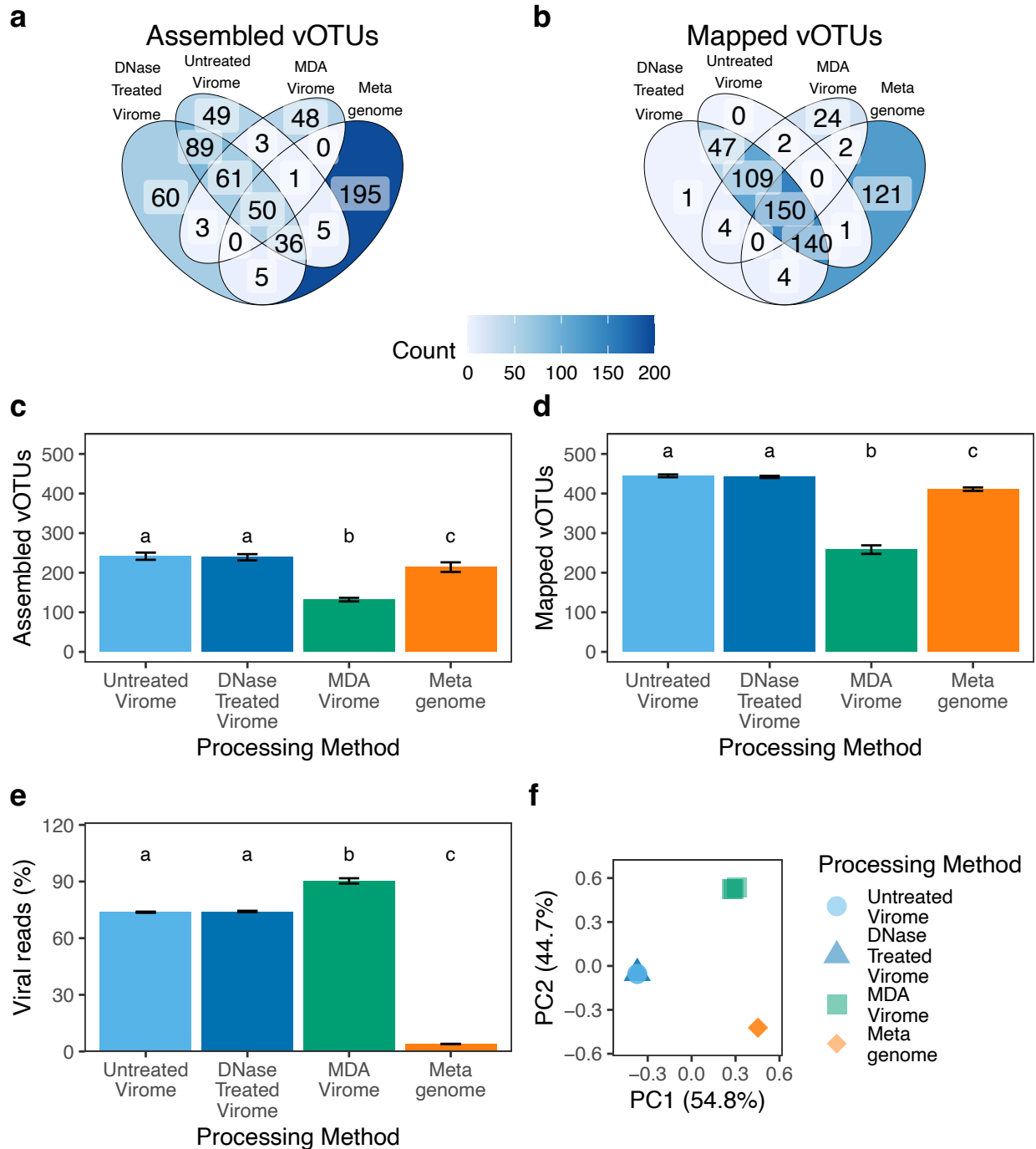
## 257 **Method-dependent impacts on vOTU recovery, proportions of viral and** 258 **rRNA gene reads, and viral community profiling**

259 To evaluate the effects of virome and metagenome preparation methods on vOTU recovery, we  
260 assessed vOTU detection using two metrics: “assembled” vOTUs or “mapped” vOTUs. Notably, vOTUs  
261 only detected via read mapping for a given processing method would not have been detected if other  
262 processing methods had not been performed to generate the reference set of 605 vOTUs, whereas

## *Processing Method Shapes Gut Virome Data*

263 “assembled” vOTUs would have been detected from that method alone (see Methods and Supplementary  
264 Fig. S3). Both metrics produced similar patterns across processing methods. DNase-treated and untreated  
265 viromes recovered highly overlapping vOTUs, with 97% shared by mapping, confirming highly similar  
266 compositions. In contrast, 50% of vOTUs assembled uniquely in MDA viromes, and 62% of vOTUs  
267 uniquely assembled in metagenomes were not detected by other methods, even after read mapping. Only  
268 25% of vOTUs were detected in at least one replicate from all four methods via read mapping (Fig. 1a-b).  
269 Metagenomes and non-MDA viromes assembled similar numbers of vOTUs (292-304), approximately  
270 half of the total, while MDA viromes only assembled 166 vOTUs (27%). By both metrics, MDA viromes  
271 shared more vOTUs with non-MDA viromes than with metagenomes, while metagenomes yielded the  
272 most unique vOTUs. These findings indicate that metagenomes and viromes recover distinct portions of  
273 the viral community, and differences persist when using a shared reference database for read mapping.

## Processing Method Shapes Gut Virome Data



274

275 *Figure 1. Comparison of vOTU recovery, read composition, and viral community structure across*

276 *methods. (a-b) Venn diagrams showing the number of vOTUs shared between methods based on (a)*

277 *assembly and (b) read mapping to a dereplicated set of 605 vOTUs. (c-d) Mean number of vOTUs*

278 *detected per library in each method by (c) assembly and (d) read mapping. (e) Percentage of reads per*

## *Processing Method Shapes Gut Virome Data*

279 *library mapped to vOTUs by method. For panels (c-e): bars = mean, error bars = standard deviation,*  
280 *letters represent groupings according to Tukey HSD where differences require  $p_{adjusted} < 0.05$ . (f) Principal*  
281 *Coordinates Analysis (PCoA) of Bray-Curtis dissimilarities between samples with percent variance*  
282 *explained by PC1 and PC2. A total of 12 samples are shown, but due to the extreme similarity between*  
283 *some, differences among technical replicates are not visible (e.g., all three metagenome samples directly*  
284 *overlap). Significant differences among methods were tested by PERMANOVA,  $R^2 = 0.996$ ,  $p < 0.001$ .*

285 Other alpha-diversity metrics support vOTU detection metrics, namely that non-MDA viromes, MDA  
286 viromes, and total metagenomes captured distinct parts of the viral community, with DNase-treated and  
287 untreated viromes statistically indistinguishable. On a per-library basis, both types of non-MDA viromes  
288 yielded significantly higher viral richness (number of vOTUs detected per library) than did MDA viromes  
289 or metagenomes by both “assembled” (Fig. 1c; ANOVA,  $F_{3,8}=85.3$ ,  $p < 0.0001$ ; Tukey HSD, all  $p_{adjusted} <$   
290  $0.001$ ) and “mapped” (Fig. 1d; ANOVA  $F_{3,8} = 31.5$ ,  $p < 0.00001$ , ; Tukey HSD, all  $p_{adjusted} < 0.01$  for non-  
291 MDA vs. MDA viromes) vOTU detection metrics. The MDA viromes had a mean of 132 assembled  
292 vOTUs, or only 55% of the vOTUs from the DNase-treated viromes from which the MDA virome DNA  
293 was sourced.

294 Despite this, MDA viromes had the highest proportion of viral reads (Fig. 1e; 91%), followed by non-  
295 MDA viromes (74% for both DNase-treated and untreated). As expected, metagenomes contained far  
296 fewer viral reads (4%; ANOVA,  $F_{3,8} = 1,720.8$ ,  $p < 0.00001$ ; Tukey  $p < 0.0001$  for all viromes vs.  
297 metagenomes). These trends were mirrored in rRNA gene read proportions (a proxy for cellular  
298 organism-derived DNA), which were highest in the metagenomes (Supplementary Fig. S4b; ANOVA,  
299  $F_{3,8} = 546.5$ ,  $p < 0.00001$ ). Human reads were slightly more abundant in the non-MDA viromes (0.22–  
300 0.25%) compared to the MDA viromes (0.14%) and metagenomes (0.12%; Supplementary Fig. S4c), but  
301 overall, these differences were not significant (ANOVA,  $F_{3,8} = 1.42$ ,  $p=0.31$ ). These results show that  
302 non-MDA viromes best recover viral diversity while minimizing cellular DNA contamination.

## *Processing Method Shapes Gut Virome Data*

303 Beta-diversity patterns based on Bray-Curtis dissimilarities clearly separated the dataset into the three  
304 methodological groups. Principal Coordinates Analysis (PCoA, Fig. 1f) revealed strong separation into  
305 three clusters corresponding to non-MDA viromes, MDA viromes, and metagenomes (PERMANOVA,  
306  $R^2 = 0.996$ ,  $p < 0.001$ ). Replicates clustered with minimal differences within methods, with DNase-treated  
307 and untreated viromes grouping together (ANOVA on distances to centroids  $F_{1,4} = 3.08$ ,  $p = 0.091$ ).  
308 Within-method dissimilarities were consistently low (0.01-0.1), while between-group dissimilarities were  
309 substantially higher (0.88-0.96), except between DNase-treated and untreated viromes (0.04;  
310 Supplementary Fig. S5). These dissimilarity values are comparable to intra-subject or between-timepoint  
311 values from previous gut virome studies (71,72), suggesting that the processing method can overshadow  
312 biological signals in viral community composition.

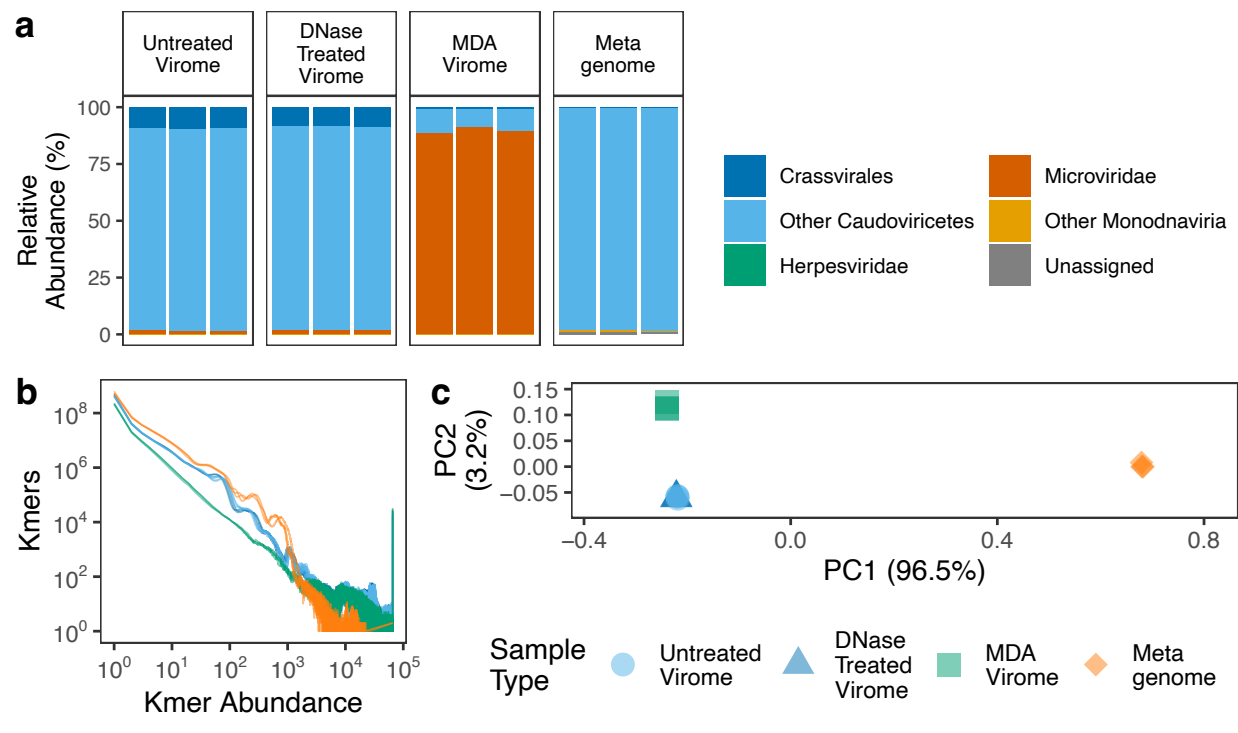
### **313 Multiple-displacement amplification severely biased viral taxonomic diversity, 314 but the biases were largely computationally correctable**

315 Despite known MDA biases, limited quantitative comparisons may contribute to the continued use of  
316 MDA viromes. To address this, we offer an empirical comparison of MDA viromes and non-MDA  
317 viromes. As expected, high-level taxonomic classification by geNomad (45) revealed that MDA viromes  
318 were overwhelmingly dominated by Microviridae, a family of small, circular, single-stranded DNA  
319 viruses, forming 90% relative abundance from 23-24 vOTUs per sample, compared to just 2% in non-  
320 MDA viromes (Fig. 2a). The staggering dominance of Microviridae in the MDA-viromes (45 times that  
321 of non-MDA viromes) bears emphasis here and adds tangible, quantitative, empirical rigor to previous  
322 suggestions of MDA bias. Conversely, the widespread dsDNA phage order Crassvirales (73), known to  
323 infect Bacteroidota and typically characterised by circular genomes of ~100 kbp (alpha-gamma families)  
324 or ~145–192 kbp (epsilon and zeta families) (74,75), was largely absent from MDA viromes (1%) and  
325 even more so from metagenomes (0.3%). In contrast, *Crassvirales* comprised 8-9% of the viral  
326 communities in non-MDA viromes, suggesting that MDA viromes may undersample this group. Since k-

## Processing Method Shapes Gut Virome Data

327 mer profiles reflect sequence diversity independently of taxonomic assignment (76–78), we also  
328 compared k-mer abundance distributions across methods to further assess how MDA affected sequence  
329 composition (Fig. 2b and Supplementary Fig. S4d). MDA viromes showed an underrepresentation of low-  
330 abundance k-mers compared to non-MDA viromes and metagenomes, consistent with lower sequence  
331 diversity in MDA viromes. Overall, MDA viromes were severely biased in recoverable viral taxonomic  
332 diversity compared to all other processing methods, leaving it difficult to justify using multiple-  
333 displacement amplification for viromics in the future if it can be avoided.

334



335

336 *Figure 2. Impact of method on viral taxonomic composition and library k-mer profiles, and demonstrated*  
337 *potential to compensate for MDA compositional biases. (a) Relative abundances of viral taxa across*  
338 *methods, based on geNomad taxonomic classifications (45). (b) K-mer abundance profiles - MDA*  
339 *viromes in green show an underrepresentation of low-abundance k-mers (left side of the plot) compared*  
340 *to high abundance k-mers (right side of the plot). (c) Principal Coordinates Analysis (PCoA) of Bray-*

## Processing Method Shapes Gut Virome Data

341 *Curtis dissimilarities after removal of ssDNA viruses and recalculation of relative abundances. Methods*  
342 *remained significantly different but with 96.5% of the variance explained by PCI, corresponding to*  
343 *differences between viromes and metagenomes (PERMANOVA, 999 iterations,  $F = 1545.2$ ,  $R^2 = 0.998$ ,  $p$*   
344 *= 0.001).*

345 To assess whether excluding ssDNA viruses mitigated MDA biases, we recalculated vOTU relative  
346 abundances after removing all ssDNA vOTUs, including the circular ssDNA families *Circoviridae*,  
347 *Genomoviridae*, *Inoviridae*, and *Microviridae*. No linear ssDNA viruses (*Spiraviridae*, *Bidnaviridae*,  
348 *Parvoviridae*) were detected. After filtering, 96.5% of the variance was attributable to differences  
349 between metagenomes and all viromes, regardless of DNase or MDA treatment (Fig. 2c). This increased  
350 observed compositional similarity across all viromes and separation of viromes from metagenomes after  
351 removing ssDNA viral data was confirmed by PERMANOVA ( $R^2 = 0.998$ ,  $p < 0.001$ ), suggesting that  
352 MDA viromes may still retain useful biological signal after dominant ssDNA vOTUs are excluded.

353 These findings highlight the substantial taxonomic distortions introduced by MDA. Still, it is  
354 encouraging that some biases can be reduced computationally to potentially make existing datasets (or  
355 future datasets if MDA is unavoidable) more representative. While MDA bias towards small circular  
356 ssDNA viruses such as *Microviridae* is known (79), our findings provide direct quantitative evidence of  
357 how this bias impacts downstream ecological interpretation and viral community structure in the human  
358 faecal virome. Although Wang et al. (21) reported similar diversity and composition between MDA  
359 viromes and non-MDA viromes, the universal use of a 3,000 bp contig cutoff likely excluded most  
360 ssDNA viruses, masking MDA biases. Our beta-diversity comparisons (Fig. 2c) confirm that such biases  
361 can be computationally addressed but not fully corrected for. Of course, as with all analyses presented  
362 here, the emphasis on comparisons across methods from the same sample does not allow for  
363 generalizability across individuals, but we have demonstrated that MDA can result in extreme bias.

364 Our findings suggest that while MDA viromes may still resolve broad compositional patterns, they  
365 remain inappropriate for detailed ecological and functional analyses, as they cannot fully compensate for

## *Processing Method Shapes Gut Virome Data*

366 the loss of diversity or sequencing depth, nor can the simple approach of removing ssDNA viral  
367 sequences. Thus, while MDA viromes may still be informative for detecting broad-scale differences in  
368 community structure, especially in samples with low viromic DNA yields and/or in re-analyses of  
369 datasets already amplified with MDA, our results suggest that using MDA in future viromic studies is  
370 difficult to justify. Where its use is unavoidable, computational corrections may help.

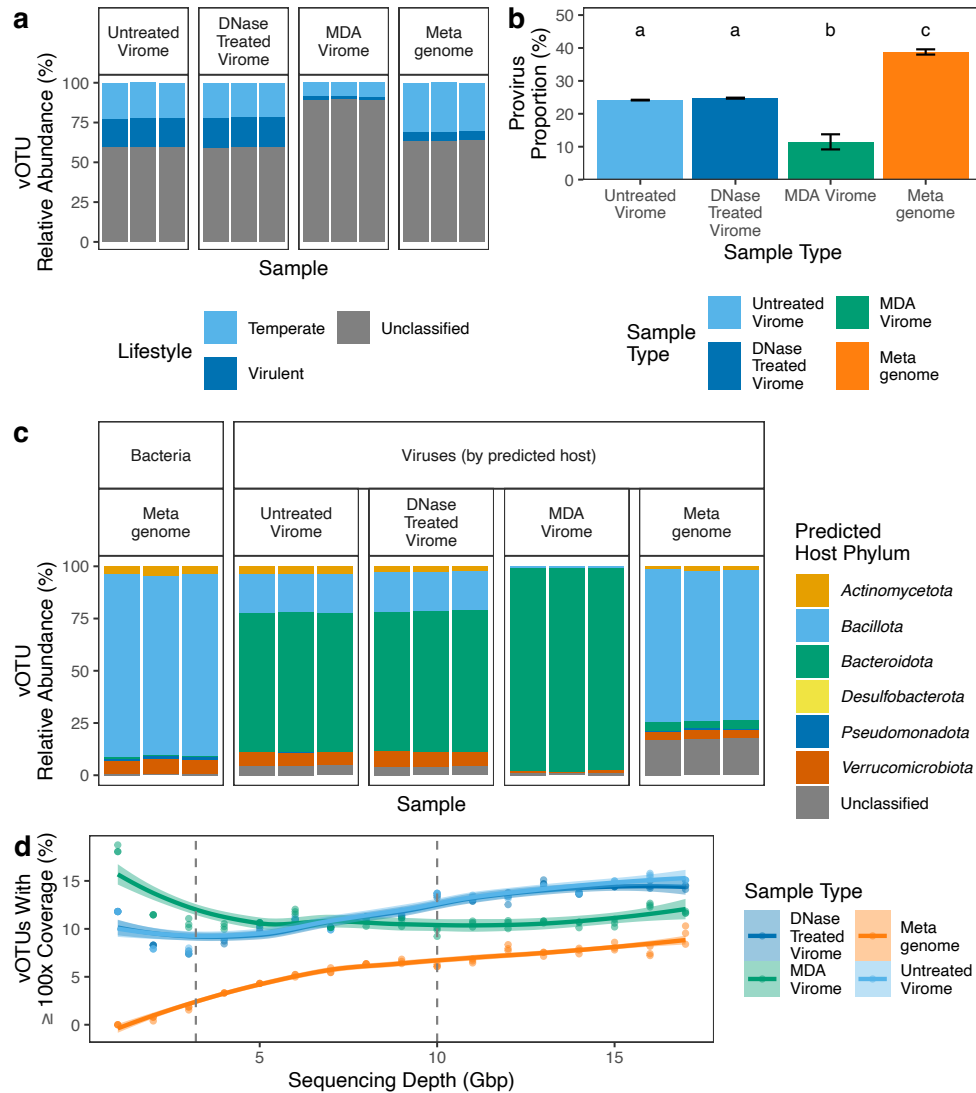
## 371 **Metagenome-derived viral communities differ from viromes in predicted** 372 **lifestyles, host associations, and genome annotations**

373 It would be logical to presume that metagenomes would recover more temperate phages (viruses  
374 capable of both lytic replication and lysogenic integration into host genomes) than viromes that target free  
375 viral particles (80,81), and here we tested that assumption and explored the differences in viral  
376 communities recovered from metagenomes and viromes. We first used BACPHLIP (62) to predict the  
377 lifestyle (temperate, virulent, or unclassified) of each vOTU, which uses a random forest-based classifier  
378 trained on the presence or absence of lysogeny-associated protein domains. Consistent with previous  
379 reports of widespread lysogeny in the human gut (79), putative temperate phages were more abundant  
380 than those predicted to be virulent across all processing methods, including viromes (Fig. 3a), suggesting  
381 that many virions recovered from viromes retain the capacity for lysogenic infection. A substantially  
382 smaller proportion of the vOTUs from MDA viromes could be assigned a putative viral lifestyle, likely  
383 due to the dominance of *Microviridae*, which are expected to be challenging for viral lifestyle prediction  
384 algorithms. Specifically, while some *Microviridae* can integrate into host genomes via co-option of host  
385 cell XerC/XerD recombinases (82), they lack phage-borne integrases or transposases, which may prevent  
386 BACPHLIP and other prediction tools from predicting a viral lifestyle. To assess the prevalence of  
387 integration specifically, we next examined the percentage of temperate phages identified as integrated  
388 prophages by geNomad, which uses a conditional random field model to detect genomic regions enriched  
389 with viral markers and flanked by host chromosomal features (45). This analysis mirrored trends from the

### *Processing Method Shapes Gut Virome Data*

390 BACPHLIP results, i.e., a lower proportion of prophages were detected in MDA viromes and a much  
391 higher proportion in metagenomes (Fig. 3b; ANOVA,  $F_{3,8} = 251.710$ ,  $p < 0.00001$ ). The detection of  
392 putative integrated prophage sequences in viromes may reflect a combination of factors, including: (1)  
393 excised host DNA packaged into virions, (2) false-positive prophage boundary predictions, (3) prophages  
394 in ultra-small bacteria that may have passed through the 0.2  $\mu\text{m}$  filter, and (4) the presence of residual  
395 host DNA/cellular contamination in VLP-concentrates (though we note that, for substantial contributions  
396 from free DNA, we would expect a difference between DNase-treated and untreated viromes, which was  
397 not observed). Overall, results suggest a greater proportion of integrated prophages recovered from the  
398 metagenomes compared to all viromes.

## Processing Method Shapes Gut Virome Data



399

400 *Figure 3. Method-dependent differences in viral lifestyle, host associations and sequencing coverage*  
 401 *depth. (a) Relative abundance of predicted viral lifestyles (temperate, virulent, or unclassified) across*  
 402 *methods, based on classification by BACPHLIP (62). (b) Percentage of temperate vOTUs predicted to be*  
 403 *prophages by geNomad (45). Bars show mean  $\pm$  standard deviation, letters indicate significant*  
 404 *differences between groups (Tukey HSD,  $p_{adjusted} < 0.05$ ). (c) vOTU relative abundances by predicted host*  
 405 *phyla, according to processing method (left) and metagenome-derived prokaryotic community*  
 406 *composition (far right).*

## Processing Method Shapes Gut Virome Data

407 We next explored whether predicted prokaryotic host taxa were similarly distributed in the viral  
408 communities recovered from each processing method and how these predicted host distributions  
409 compared to the prokaryotic community compositions recovered from the metagenomes. Hosts for each  
410 vOTU were predicted using iPHoP, and bacterial community profiles were characterised by SingleM  
411 (38,63) (Fig. 3c). Bacterial communities were dominated by *Bacillota* (formerly *Firmicutes* (83)), a  
412 pattern reflected in the predicted host associations of vOTUs identified in the metagenomes but not the  
413 viromes. This is consistent with the observed greater proportion of predicted prophages in the  
414 metagenomes compared to viromes, as viral and host abundance should be more highly correlated in the  
415 metagenomes, where they are more often coming from the same chromosome. Although viromes and  
416 metagenomes generally yielded comparable numbers of vOTUs predicted to infect each bacterial phylum,  
417 the relative abundance distributions of these vOTUs differed substantially across processing methods. For  
418 example, phages predicted to infect the phylum *Bacillota* comprised 72% of the viral community by  
419 relative abundance in metagenomes but only 19% in DNase-treated viromes, despite comparable  
420 proportions by vOTU counts (60% and 51%, respectively). In contrast, viruses predicted to infect the  
421 phylum *Bacteroidota* dominated all viromes (67% relative abundance of non-MDA viromes, 97% of  
422 MDA viromes) but were rare in metagenome viral communities (4%) and virtually absent in the  
423 prokaryotic communities (0.7%). Together, these results suggest that different processing methods could  
424 lead to wildly different interpretations of infection dynamics, since viral relative abundances differed  
425 dramatically between viromes and metagenomes when grouped according to predicted hosts.

426 We compared profiles of functionally annotated viral genes, including putative auxiliary metabolic  
427 genes (AMGs) (1), across processing methods. To more fully capture viral gene content, analyses were  
428 conducted at the assembled contig (as opposed to vOTU) level, after meeting viral prediction thresholds  
429 (see Methods). Using Pharokka (61), we found that 0.9-1.3% of genes across all viral contigs were  
430 annotated as moron elements (transferable elements within phage genomes (84)), accessory metabolic  
431 genes, or were involved in host takeover, with no significant differences across viromic methods (Tukey

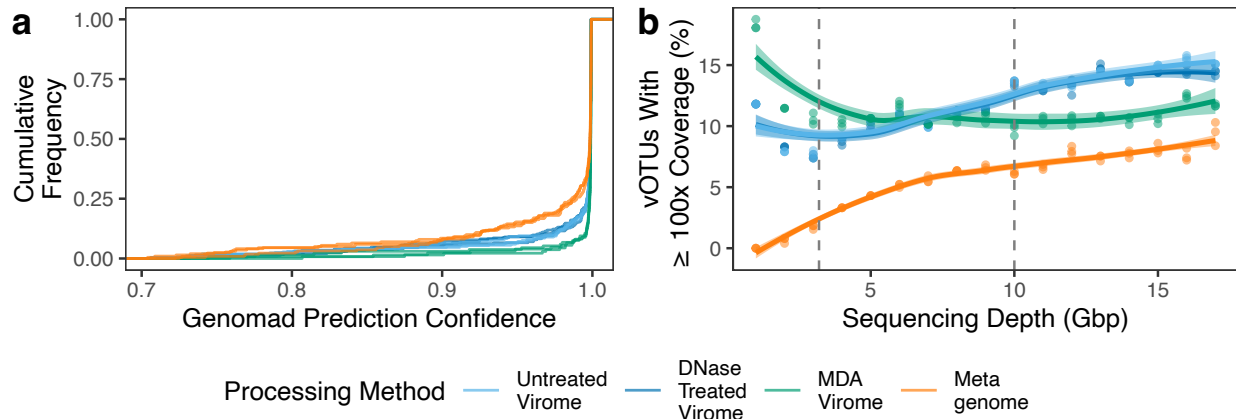
## *Processing Method Shapes Gut Virome Data*

432 HSD,  $p > 0.05$ ). However, this category of gene was ~33% more frequently detected in metagenome-  
433 derived viral contigs compared to those from DNase-treated viromes (Supplementary Fig. S6a),  
434 suggesting greater prevalence in host-associated viral genomes (e.g., in integrated or actively replicating  
435 viruses), as previously suggested (1), and/or more false-positive viral predictions or errors predicting  
436 prophage boundaries in metagenomes. Accessory genes were rare overall, with significant differences  
437 only between viromes and metagenomes. This overrepresentation in metagenome-derived viral contigs  
438 may reflect false-positive detection of host-derived sequences rather than true viral gene content, and  
439 underscores the need for rigorous quality control when analysing putative AMGs (85,86).

## 440 **Methodological Impact on Viral Prediction Confidence and Viral Recovery at** 441 **Increasing Sequencing Depths**

442 To assess whether vOTU quality might contribute to observed differences between viromes and  
443 metagenomes, we next examined viral prediction confidence scores across processing methods. geNomad  
444 confidence scores differed significantly (Fig. 4a, ANOVA,  $F_{3,8} = 47.5$ ,  $p = 1.92 \times 10^{-5}$ ), but the mean shift  
445 between processing methods was only a modest shift of 0.8–1.7%. Cumulative frequency diagrams (Fig.  
446 4a) show that metagenomes contain a greater proportion of lower-confidence viral contigs, underscoring  
447 the need for additional caution when analysing metagenome-derived viral sequences, as a small shift in  
448 confidence score distribution can result in the inclusion of tens to hundreds of lower-quality viral  
449 sequences. Conversely, 2,261 contigs were excluded through length-filtering but had viral confidence  
450 scores  $>0.95$ . These shorter, high-confidence contigs may still be useful in specific contexts, but this  
451 choice must be clearly justified to avoid inclusion of false positives.

## Processing Method Shapes Gut Virome Data



452

453 *Figure 4. Impact of processing method on viral prediction and high-coverage viral contigs. (a)*

454 *Cumulative frequency diagram of geNomad prediction confidence scores of viral contigs filtered for*

455 *length  $\geq 10$  Kbp or between 1 and 10 Kbp and geNomad assigned phylum = Monodnaviria. (b) Number*

456 *of vOTUs with  $\geq 100\times$  coverage across subsampled sequencing depths (Gbp) for each method. Lines and*

457 *shaded areas indicate fitted LOESS curves with 95% confidence intervals. Dashed vertical lines indicate*

458 *commonly used viral dataset sequencing targets, 3.2 Gbp (56) and 10 Gbp (69,87–89)*

459 One presumed advantage of viromes over metagenomes is improved recovery of strain-level

460 microdiversity, which requires high coverage depth (90,91). To compare coverage depth for vOTUs

461 across processing methods and sequencing effort, we subsampled the raw reads from each library in 1

462 Gbp increments between 1 and 17 Gbp and reprocessed each subset independently. Metagenomes

463 consistently had the lowest proportion of vOTUs with  $\geq 100\times$  average coverage (Fig. 4b), indicating, as

464 expected, that viromic methods offer better access to sufficient coverage depth for strain-level analyses.

465 At depths  $< 7$  Gbp, MDA viromes outperformed non-MDA viromes in recovering high-coverage contigs,

466 reflecting lower viral diversity in MDA viromes and leading to higher coverage. However, this trend was

467 reversed at higher sequencing efforts, with non-MDA viromes consistently capturing vOTUs with higher

468 coverage. In non-MDA viromes, high-coverage vOTUs plateaued at  $\leq 14\%$  of all vOTUs after 12.5 Gbp,

469 suggesting that per-sample strain-level analyses would likely only be possible for high-abundance

## *Processing Method Shapes Gut Virome Data*

470 vOTUs. Our results further confirm that non-MDA viromes outperform both metagenomes and MDA  
471 viromes in generating high-coverage vOTUs suitable for detailed strain-level analyses.

### 472 **The majority of recovered vOTUs were absent from existing human gut** 473 **virome databases**

474 The extent to which existing reference databases capture gut virome diversity is unknown, limiting  
475 our understanding of the human gut virosphere. To assess the novelty of viruses recovered by this study  
476 according to processing method, we clustered all 2,480 recovered viral contigs with the Unified Human  
477 Gut Virome catalogue (UHGV, <https://github.com/snayfach/UHGV> - accessed June 12<sup>th</sup> 2025), a non-  
478 redundant set of 168,536 vOTUs from 12 large-scale datasets (31,49,51–60). Species-level clustering  
479 yielded 603 vOTU clusters containing at least one viral contig from this study, compared to 605 vOTUs  
480 formed from our study alone. Only 35% (214 of 603) of clusters included UHGV sequences, meaning  
481 65% of our recovered vOTUs were not present in the reference database (Supplementary Fig. S7). Read-  
482 mapping to the UHGV database identified a further 248 UHGV vOTUs that were not assembled *de novo*  
483 here (Supplementary Fig. S7c), with non-MDA viromes detecting 17% more than metagenomes and  
484 130% more than MDA viromes (Supplementary Fig. S7d). These mapped-only vOTUs had similar  
485 coverage (Supplementary Fig. S7e) but were, on average, 50% shorter in length than clustered vOTUs  
486 (Supplementary Fig. S7f). These vOTUs may represent viral genomes with intrinsic features, such as high  
487 microdiversity or repetitive elements, that hinder complete assembly. Consistent with previous studies  
488 (2), our results indicate that a substantial fraction of human gut viral diversity remains uncharacterised  
489 and that non-MDA viromes best recover low-abundance viruses, both novel and reference-mapped but  
490 unassembled vOTUs.

491

## *Processing Method Shapes Gut Virome Data*

### 492 **Conclusions and outlook**

493 We demonstrate how methodological choices in faecal DNA preparation can shape the composition  
494 of the recovered gut viral community and downstream interpretations. MDA introduced a striking bias  
495 toward *Microviridae*, consistent with prior studies of ssDNA overamplification (23–25,92–95). Although  
496 computationally filtering out short ssDNA contigs can reduce this distortion, MDA remains unsuitable for  
497 more detailed ecological comparisons. Viromes had higher viral richness, fewer putative temperate  
498 phages (viruses capable of switching between lytic replication and lysogeny), and fewer integrated  
499 prophages than metagenomes, emphasising the need to align methodological choices with study  
500 objectives.

501 We also showed that differences in viral community composition due to preparation methods can  
502 propagate through downstream analyses beyond community diversity metrics, with the potential for  
503 substantially influencing ecological and functional conclusions. We applied a suite of commonly used  
504 analytical approaches to examine how methodological choice affected interpretation, resulting in an  
505 analytical framework that could be useful for future methodological comparisons. For example, MDA  
506 viromes yielding fewer lifestyle predictions due to *Microviridae* dominance, and metagenomes showed  
507 substantially different predicted host compositions of the viral community at the phylum level compared  
508 to both non-MDA and MDA viromes. Had each method been used in separate studies, these differences  
509 could have led to conflicting interpretations, as they produce methodological artefacts that can be difficult  
510 to recognise in the literature without expert technical evaluation of study methodologies (19,96,97).  
511 Despite the study's limited scope, the consistency across replicates and the magnitude of the observed  
512 effects emphasise the importance of understanding the sources of methodological bias and potential  
513 mitigation methods. The more refined methods described herein will have significant value when applied  
514 to larger-scale human studies that explore interindividual variability of the gut virome and associations of  
515 the virome with health phenotypes.

## *Processing Method Shapes Gut Virome Data*

516 Our findings complement and extend prior gut virome methods comparisons, which have often  
517 focused on individual steps, such as viral enrichment, DNA extraction, and sequencing library  
518 construction (15,19,21,30,98,99). No single method can capture all aspects of gut viral diversity, but by  
519 understanding the specific biases and strengths of each technique, researchers can make more informed  
520 methodological choices. As larger-scale, more integrative and multi-omic studies become more prevalent,  
521 careful method selection will become increasingly essential for generating robust insights into the role of  
522 the gut virome in human health and disease.

## 523 **Acknowledgments**

524 Elements of the graphical abstract and Supplementary Fig. S1 were produced in BioRender. The  
525 sequencing was carried by the DNA Technologies and Expression Analysis Core at the UC Davis  
526 Genome Center, supported by NIH Shared Instrumentation Grant 1S10OD010786-01. The authors also  
527 thank other members of the Emerson Lab for helpful discussions and general feedback.

## 528 **Authors' contributions**

529 LSH: conceptualisation, data curation, formal analysis, writing – original draft preparation, visualization  
530 TAK: resources, project administration, writing – review and editing  
531 SHA: resources, project administration, writing – review and editing  
532 MRA: resources, project administration, writing – review and editing  
533 MO: conceptualisation, formal analysis, visualization, writing – review and editing  
534 JBE: conceptualisation, wet-lab methodology, investigation, writing – review and editing, supervision,  
535 funding acquisition, project administration

536

## *Processing Method Shapes Gut Virome Data*

### 537 **Funding**

538 This research was supported by the NIH Common Fund (Human Virome Program), Award #  
539 U01DE034198. LSH was also partially supported by the U.S. Department of Energy (DOE), Office of  
540 Science, Office of Biological and Environmental Research (BER), Genomic Science Program, award  
541 number DE-SC0023127 (grant to JBE, grant PI Sydney Glassman). Research on the human microbiome  
542 by Drs. Adams, Knotts, and Ali is funded, in part, by NIH-NIDDK 1R01DK137173-01A1.

### 543 **Data and Code Availability**

544 All raw sequencing data have been deposited with the SRA under BioProject PRJNA1331857  
545 (SRR35523994 - SRR35524005). As sequencing data deposition requires the removal of human  
546 metagenomic reads, human reads were scrubbed from the raw read files with the NCBI's Human Read  
547 Removal Tool (<https://hub.docker.com/r/ncbi/sra-human-scrubber>) prior to submission. Human read  
548 count tables are archived in the GitHub and Zenodo repositories. All filtered viral sequences were  
549 deposited in GenBank and in the GitHub/Zenodo repositories for the manuscript. All R scripts involved in  
550 the processing and analysis of these data, plus summary tables used as input, have been deposited on  
551 GitHub (<https://github.com/LSHillary/FecalViromeOptimisation>) and archived on Zenodo (DOI:  
552 10.5281/zenodo.17527407).

### 553 **Competing interests**

554 S.H. Adams is founder and principal of XenoMed, LLC (dba XenoMet), which is focused on research and  
555 discovery in microbial metabolism. XenoMed had no part in the research design, funding, results or  
556 writing of the manuscript.

557

## *Processing Method Shapes Gut Virome Data*

### 558 **References**

- 559 1. Luo XQ, Wang P, Li JL, Ahmad M, Duan L, Yin LZ, et al. Viral community-wide auxiliary  
560 metabolic genes differ by lifestyles, habitats, and hosts. *Microbiome*. 2022 Nov 5;10(1):190.
- 561 2. Shkoporov AN, Clooney AG, Sutton TDS, Ryan FJ, Daly KM, Nolan JA, et al. The Human Gut  
562 Virome Is Highly Diverse, Stable, and Individual Specific. *Cell Host Microbe*. 2019 Oct 9;26(4):527-  
563 541.e5.
- 564 3. Cao Z, Sugimura N, Burgermeister E, Ebert MP, Zuo T, Lan P. The gut virome: A new microbiome  
565 component in health and disease. *eBioMedicine*. 2022 July 1;81:104113.
- 566 4. Liang G, Cobián-Güemes AG, Albenberg L, Bushman F. The gut virome in inflammatory bowel  
567 diseases. *Curr Opin Virol*. 2021 Dec 1;51:190–8.
- 568 5. Ungaro F, Massimino L, Furfaro F, Rimoldi V, Peyrin-Biroulet L, D’Alessio S, et al. Metagenomic  
569 analysis of intestinal mucosa revealed a specific eukaryotic gut virome signature in early-diagnosed  
570 inflammatory bowel disease. *Gut Microbes*. 2019 Mar 4;10(2):149–58.
- 571 6. Zhang P, Shi H, Guo R, Li L, Guo X, Yang H, et al. Metagenomic analysis reveals altered gut virome  
572 and diagnostic potential in pancreatic cancer. *J Med Virol*. 2024 July 1;96(7):e29809.
- 573 7. Federici S, Kredon-Russo S, Valdés-Mas R, Kviatcovsky D, Weinstock E, Matiuhin Y, et al. Targeted  
574 suppression of human IBD-associated gut microbiota commensals by phage consortia for treatment  
575 of intestinal inflammation. *Cell*. 2022 Aug 4;185(16):2879-2898.e24.
- 576 8. Mao X, Larsen SB, Zachariassen LSF, Brunse A, Adamberg S, Mejia JLC, et al. Transfer of modified  
577 gut viromes improves symptoms associated with metabolic syndrome in obese male mice. *Nat*  
578 *Commun*. 2024 June 3;15(1):4704.
- 579 9. Breitbart Mya, Hewson Ian, Felts Ben, Mahaffy Joseph M., Nulton James, Salamon Peter, et al.  
580 Metagenomic Analyses of an Uncultured Viral Community from Human Feces. *J Bacteriol*. 2003 Oct  
581 15;185(20):6220–3.
- 582 10. Li J, Yang F, Xiao M, Li A. Advances and challenges in cataloging the human gut virome. *Cell Host*  
583 *Microbe*. 2022 July 13;30(7):908–16.
- 584 11. Stockdale SR, Hill C. Progress and prospects of the healthy human gut virome. *Curr Opin Virol*.  
585 2021 Dec 1;51:164–71.
- 586 12. Halary S, Temmam S, Raoult D, Desnues C. Viral metagenomics: are we missing the giants? *Environ*  
587 *Microbiol Spec Sect Megaviromes*. 2016 June 1;31:34–43.
- 588 13. Santos-Medellin C, Zinke LA, ter Horst AM, Gelardi DL, Parikh SJ, Emerson JB. Viromes  
589 outperform total metagenomes in revealing the spatiotemporal patterns of agricultural soil viral  
590 communities. *ISME J*. 2021;15:1956–1970.
- 591 14. Trubl G, Hyman P, Roux S, Abedon ST. Coming-of-age characterization of soil viruses: A user’s  
592 guide to virus isolation, detection within metagenomes, and viromics. *Soil Syst*. 2020;4(2):1–34.

## *Processing Method Shapes Gut Virome Data*

- 593 15. Kosmopoulos JC, Klier KM, Langwig MV, Tran PQ, Anantharaman K. Viromes vs. mixed  
594 community metagenomes: choice of method dictates interpretation of viral community ecology.  
595 *Microbiome*. 2024 Oct 7;12(1):195.
- 596 16. Shkoporov AN, Ryan FJ, Draper LA, Forde A, Stockdale SR, Daly KM, et al. Reproducible  
597 protocols for metagenomic analysis of human faecal phageomes. *Microbiome*. 2018 Apr 10;6(1):68.
- 598 17. d’Humières C, Touchon M, Dion S, Cury J, Ghazlane A, Garcia-Garcera M, et al. A simple,  
599 reproducible and cost-effective procedure to analyse gut phageome: from phage isolation to  
600 bioinformatic approach. *Sci Rep*. 2019 Aug 5;9(1):11331.
- 601 18. Kleiner M, Hooper LV, Duerkop BA. Evaluation of methods to purify virus-like particles for  
602 metagenomic sequencing of intestinal viromes. *BMC Genomics*. 2015 Jan 22;16(1):7.
- 603 19. Callanan J, Stockdale SR, Shkoporov A, Draper LA, Ross RP, Hill C. Biases in Viral Metagenomics-  
604 Based Detection, Cataloguing and Quantification of Bacteriophage Genomes in Human Faeces, a  
605 Review. *Microorganisms*. 2021;9(3).
- 606 20. Hsieh SY, Tariq MA, Telatin A, Ansorge R, Adriaenssens EM, Savva GM, et al. Comparison of PCR  
607 versus PCR-Free DNA Library Preparation for Characterising the Human Faecal Virome. *Viruses*.  
608 2021;13(10).
- 609 21. Wang G, Li S, Yan Q, Guo R, Zhang Y, Chen F, et al. Optimization and evaluation of viral  
610 metagenomic amplification and sequencing procedures toward a genome-level resolution of the  
611 human fecal DNA virome. *J Adv Res*. 2023 June 1;48:75–86.
- 612 22. Zhai X, Gobbi A, Kot W, Krych L, Nielsen DS, Deng L. A single-stranded based library preparation  
613 method for virome characterization. *Microbiome*. 2024 Oct 24;12(1):219.
- 614 23. Binga EK, Lasken RS, Neufeld JD. Something from (almost) nothing: the impact of multiple  
615 displacement amplification on microbial ecology. *ISME J*. 2008 Mar 1;2(3):233–41.
- 616 24. Kim KH, Bae JW. Amplification methods bias metagenomic libraries of uncultured single-stranded  
617 and double-stranded DNA viruses. *Appl Environ Microbiol*. 2011;77(21):7663--7668.
- 618 25. Parras-Molto M, Rodriguez-Galet A, Suarez-Rodriguez P, Lopez-Bueno A. Evaluation of bias  
619 induced by viral enrichment and random amplification protocols in metagenomic surveys of saliva  
620 DNA viruses. *Microbiome*. 2018;6(1):119.
- 621 26. Emerson JB, Thomas BC, Andrade K, Allen EE, Heidelberg KB, Banfield JF. Dynamic Viral  
622 Populations in Hypersaline Systems as Revealed by Metagenomic Assembly. *Appl Environ*  
623 *Microbiol*. 2012 Sept;78(17):6309–20.
- 624 27. Geonczy SE, Hillary LS, Santos-Medellín C, Fudyma JD, Sorensen JW, Emerson JB. Virome  
625 responses to heating of a forest soil suggest that most dsDNA viral particles do not persist at 90°C.  
626 *Soil Biol Biochem*. 2025 Mar 1;202:109651.
- 627 28. Sorensen JW, Zinke LA, ter Horst AM, Santos-Medellin C, Schroeder A, Emerson JB. DNase  
628 Treatment Improves Viral Enrichment in Agricultural Soil Viromes. *mSystems*. 2021;6(5):e00614-  
629 21.

## *Processing Method Shapes Gut Virome Data*

- 630 29. Guan, Huihui, Pu, Yanni, Liu, Chenglin, Lou, Tao, Tan, Shishang, Kong, Mengmeng, et al.  
631 Comparison of Fecal Collection Methods on Variation in Gut Metagenomics and Untargeted  
632 Metabolomics. *mSphere*. 2021 Sept 15;6(5):10.1128/msphere.00636-21.
- 633 30. Conceição-Neto N, Zeller M, Lefrère H, De Bruyn P, Beller L, Deboutte W, et al. Modular approach  
634 to customise sample preparation procedures for viral metagenomics: a reproducible protocol for  
635 virome analysis. *Sci Rep*. 2015 Nov 12;5(1):16532.
- 636 31. Gregory AC, Zablocki O, Zayed AA, Howell A, Bolduc B, Sullivan MB. The Gut Virome Database  
637 Reveals Age-Dependent Patterns of Virome Diversity in the Human Gut. *Cell Host Microbe*. 2020  
638 Nov 11;28(5):724-740.e8.
- 639 32. Pavlopoulos GA, Baltoumas FA, Liu S, Selvitopi O, Camargo AP, Nayfach S, et al. Unraveling the  
640 functional dark matter through global metagenomics. *Nature*. 2023 Oct 1;622(7983):594–602.
- 641 33. Zhang L, Chen F, Zeng Z, Xu M, Sun F, Yang L, et al. Advances in Metagenomics and Its  
642 Application in Environmental Microorganisms. *Front Microbiol*. 2021;12:766364.
- 643 34. World Medical Association. World Medical Association Declaration of Helsinki: Ethical Principles  
644 for Medical Research Involving Human Participants. *JAMA*. 2025 Jan 7;333(1):71–4.
- 645 35. Santos-Medellín C, Blazewicz SJ, Pett-Ridge J, Firestone MK, Emerson JB. Viral but not bacterial  
646 community successional patterns reflect extreme turnover shortly after rewetting dry soils. *Nat Ecol  
647 Evol*. 2023 Nov;7(11):1809–22.
- 648 36. Crusoe MR, Alameldin HF, Awad S, Boucher E, Caldwell A, Cartwright R, et al. The khmer  
649 software package: enabling efficient nucleotide sequence analysis [Internet]. *F1000Research*; 2015  
650 [cited 2024 Feb 23]. Available from: <https://f1000research.com/articles/4-900>
- 651 37. Kopylova E, Noe L, Touzet H. SortMeRNA: fast and accurate filtering of ribosomal RNAs in  
652 metatranscriptomic data. *Bioinformatics*. 2012;28(24):3211--3217.
- 653 38. Woodcroft BJ, Aroney STN, Zhao R, Cunningham M, Mitchell JAM, Nurdiansyah R, et al.  
654 Comprehensive taxonomic identification of microbial species in metagenomic data using SingleM  
655 and Sandpiper. *Nat Biotechnol* [Internet]. 2025 July 16; Available from:  
656 <https://doi.org/10.1038/s41587-025-02738-1>
- 657 39. Nurk S, Koren S, Rhie A, Rautiainen M, Bzikadze AV, Mikheenko A, et al. The complete sequence  
658 of a human genome. *Science*. 2022 Apr;376(6588):44–53.
- 659 40. Li H. Minimap2: pairwise alignment for nucleotide sequences. *Bioinformatics*. 2018 Sept  
660 15;34(18):3094–100.
- 661 41. Li H, Handsaker B, Wysoker A, Fennell T, Ruan J, Homer N, et al. The Sequence Alignment/Map  
662 format and SAMtools. *Bioinformatics*. 2009 Aug 15;25(16):2078–9.
- 663 42. Aroney STN, Newell RJP, Nissen JN, Camargo AP, Tyson GW, Woodcroft BJ. CoverM: read  
664 alignment statistics for metagenomics. *Bioinformatics*. 2025 Apr 1;41(4):btaf147.

## *Processing Method Shapes Gut Virome Data*

- 665 43. Li D, Liu CM, Luo R, Sadakane K, Lam TW. MEGAHIT: an ultra-fast single-node solution for large  
666 and complex metagenomics assembly via succinct de Bruijn graph. *Bioinformatics*.  
667 2015;31(10):1674--1676.
- 668 44. Mikheenko A, Prjibelski A, Saveliev V, Antipov D, Gurevich A. Versatile genome assembly  
669 evaluation with QUAST-LG. *Bioinformatics*. 2018 July 1;34(13):i142–50.
- 670 45. Camargo AP, Roux S, Schulz F, Babinski M, Xu Y, Hu B, et al. Identification of mobile genetic  
671 elements with geNomad. *Nat Biotechnol*. 2024 Aug;42:1303–12.
- 672 46. Roux S, Adriaenssens EM, Dutilh BE, Koonin EV, Kropinski AM, Krupovic M, et al. Minimum  
673 Information about an Uncultivated Virus Genome (MIUViG). *Nat Biotechnol*. 2018;37(1):29–37.
- 674 47. Krupovic M. Networks of evolutionary interactions underlying the polyphyletic origin of ssDNA  
675 viruses. *Curr Opin Virol*. 2013 Oct 1;3(5):578–86.
- 676 48. Morgulis A, Coulouris G, Raytselis Y, Madden TL, Agarwala R, Schäffer AA. Database indexing for  
677 production MegaBLAST searches. *Bioinformatics*. 2008 Aug 15;24(16):1757–64.
- 678 49. Camargo AP, Nayfach S, Chen IMA, Palaniappan K, Ratner A, Chu K, et al. IMG/VR v4: an  
679 expanded database of uncultivated virus genomes within a framework of extensive functional,  
680 taxonomic, and ecological metadata. *Nucleic Acids Res*. 2023 Jan 6;51(D1):D733–43.
- 681 50. Nayfach S, Camargo AP, Schulz F, Eloë-Fadrosh E, Roux S, Kyrpides NC. CheckV assesses the  
682 quality and completeness of metagenome-assembled viral genomes. *Nat Biotechnol*. 2020;39(5):578-  
683 -585.
- 684 51. Benler S, Yutin N, Antipov D, Rayko M, Shmakov S, Gussow AB, et al. Thousands of previously  
685 unknown phages discovered in whole-community human gut metagenomes. *Microbiome*. 2021 Mar  
686 29;9(1):1–17.
- 687 52. Camarillo-Guerrero LF, Almeida A, Rangel-Pineros G, Finn RD, Lawley TD. Massive expansion of  
688 human gut bacteriophage diversity. *Cell*. 2021 Feb 18;184(4):1098-1109.e9.
- 689 53. Garmeva S, Gulyaeva A, Sinha T, Shkoporov AN, Clooney AG, Stockdale SR, et al. Stability of the  
690 human gut virome and effect of gluten-free diet. 2021 May 18;34:109132.
- 691 54. Lai S, Jia L, Subramanian B, Pan S, Zhang J, Dong Y, et al. mMGE: a database for human  
692 metagenomic extrachromosomal mobile genetic elements. *Nucleic Acids Res*. 2021 Jan  
693 8;49(D1):D783–91.
- 694 55. Carter MM, Olm MR, Merrill BD, Dahan D, Tripathi S, Spencer SP, et al. Ultra-deep sequencing of  
695 Hadza hunter-gatherers recovers vanishing gut microbes. *Cell*. 2023 July 6;186(14):3111-3124.e13.
- 696 56. Nayfach S, Páez-Espino D, Call L, Low SJ, Sberro H, Ivanova NN, et al. Metagenomic compendium  
697 of 189,680 DNA viruses from the human gut microbiome. *Nat Microbiol*. 2021 July 1;6(7):960–70.
- 698 57. Shah SA, Deng L, Thorsen J, Pedersen AG, Dion MB, Castro-Mejía JL, et al. Expanding known viral  
699 diversity in the healthy infant gut. *Nat Microbiol*. 2023 May 1;8(5):986–98.

## *Processing Method Shapes Gut Virome Data*

- 700 58. Soto-Perez P, Bisanz JE, Berry JD, Lam KN, Bondy-Denomy J, Turnbaugh PJ. CRISPR-Cas System  
701 of a Prevalent Human Gut Bacterium Reveals Hyper-targeting against Phages in a Human Virome  
702 Catalog. 2019 Sept 11;26:325–35.
- 703 59. Tisza MJ, Buck CB. A catalog of tens of thousands of viruses from human metagenomes reveals  
704 hidden associations with chronic diseases. *Proc Natl Acad Sci*. 2021 June 8;118(23):e2023202118.
- 705 60. Van Espen L, Bak EG, Beller L, Close L, Deboutte W, Juel HB, et al. A Previously Undescribed  
706 Highly Prevalent Phage Identified in a Danish Enteric Virome Catalog. *mSystems*. 2021 Oct  
707 19;6(5):10.1128/msystems.00382-21.
- 708 61. Bouras G, Nepal R, Houtak G, Psaltis AJ, Wormald PJ, Vreugde S. Pharokka: a fast scalable  
709 bacteriophage annotation tool. *Bioinformatics*. 2023 Jan 1;39(1):btac776.
- 710 62. Hockenberry AJ, Wilke CO. BACPHLIP: predicting bacteriophage lifestyle from conserved protein  
711 domains. *Breitbart M, editor. PeerJ*. 2021 May 6;9:e11396.
- 712 63. Roux S, Camargo AP, Coutinho FH, Dabdoub SM, Dutilh BE, Nayfach S, et al. iPHoP: An  
713 integrated machine learning framework to maximize host prediction for metagenome-derived viruses  
714 of archaea and bacteria. *PLOS Biol*. 2023 Apr 21;21(4):e3002083.
- 715 64. Kassambara A. ggpubr: ‘ggplot2’ Based Publication Ready Plots [Internet]. 2020. Available from:  
716 <https://CRAN.R-project.org/package=ggpubr>
- 717 65. Wickham H, Averick M, Bryan J, Chang W, McGowan LD, François R, et al. Welcome to the  
718 tidyverse. *J Open Source Softw*. 2019;4(43):1686.
- 719 66. Graves S, Piepho HP, Selzer ML. Package ‘multcompView’. *Vis Paired Comp*. 2015;451:452.
- 720 67. Gao CH, Chen C, Akyol T, Dusa A, Yu G, Cao B, et al. ggVennDiagram: Intuitive Venn diagram  
721 software extended. *iMeta*. 2024;3(1):e177.
- 722 68. Oksanen J, Blanchet FG, Friendly M, Kindt R, Legendre P, McGlinn D, et al. vegan: Community  
723 Ecology Package. 2019; Available from: <https://cran.r-project.org/package=vegan>
- 724 69. Santos-Medellín C, Estera-Molina K, Yuan M, Pett-Ridge J, Firestone MK, Emerson JB. Spatial  
725 turnover of soil viral populations and genotypes overlain by cohesive responses to moisture in  
726 grasslands. *Proc Natl Acad Sci*. 2022 Nov 8;119(45):e2209132119.
- 727 70. Shimada O, Ishikawa H, Tosaka-Shimada H, Yasuda T, Kishi K, Suzuki S. Detection of  
728 deoxyribonuclease I along the secretory pathway in paneth cells of human small intestine. *J*  
729 *Histochem Cytochem*. 1998;46(7):833–40.
- 730 71. Yan A, Butcher J, Mack D, Stintzi A. Virome Sequencing of the Human Intestinal Mucosal–Luminal  
731 Interface. *Front Cell Infect Microbiol*. 2020 Oct 22;10:582187.
- 732 72. Zeng S, Almeida A, Li S, Ying J, Wang H, Qu Y, et al. A metagenomic catalog of the early-life  
733 human gut virome. *Nat Commun*. 2024 Feb 29;15(1):1864.

## *Processing Method Shapes Gut Virome Data*

- 734 73. Smith L, Goldobina E, Govi B, Shkoporov AN. Bacteriophages of the Order Crassvirales: What Do  
735 We Currently Know about This Keystone Component of the Human Gut Virome? *Biomolecules*.  
736 2023 Mar 24;13(4):584.
- 737 74. Guerin E, Shkoporov A, Stockdale SR, Clooney AG, Ryan FJ, Sutton TDS, et al. Biology and  
738 Taxonomy of crAss-like Bacteriophages, the Most Abundant Virus in the Human Gut. *Cell Host*  
739 *Microbe*. 2018 Nov 14;24(5):653-664.e6.
- 740 75. Yutin N, Benler S, Shmakov SA, Wolf YI, Tolstoy I, Rayko M, et al. Analysis of metagenome-  
741 assembled viral genomes from the human gut reveals diverse putative CrAss-like phages with unique  
742 genomic features. *Nat Commun*. 2021 Feb 16;12(1):1044.
- 743 76. Bokulich NA. Integrating sequence composition information into microbial diversity analyses with k-  
744 mer frequency counting. *mSystems*. 2025 Feb 20;10(3):e01550-24.
- 745 77. Dubinkina VB, Ischenko DS, Ulyantsev VI, Tyakht AV, Alexeev DG. Assessment of k-mer spectrum  
746 applicability for metagenomic dissimilarity analysis. *BMC Bioinformatics*. 2016 Jan 16;17(1):1–11.
- 747 78. Jenike KM, Campos-Domínguez L, Boddé M, Cerca J, Hodson CN, Schatz MC, et al. k-mer  
748 approaches for biodiversity genomics. *Genome Res*. 2025 Jan 2;35(2):219–30.
- 749 79. Kim MS, Bae JW. Lysogeny is prevalent and widely distributed in the murine gut microbiota. *ISME*  
750 *J*. 2018 Apr 1;12(4):1127–41.
- 751 80. Sbardellati DL, Vannette RL. Targeted viromes and total metagenomes capture distinct components  
752 of bee gut phage communities. *Microbiome*. 2024 Aug 23;12(1):155.
- 753 81. Sommers P, Chatterjee A, Varsani A, Trubl G. Integrating Viral Metagenomics into an Ecological  
754 Framework. *Annu Rev Virol*. 2021;8(1):133--158.
- 755 82. Krupovic M, Forterre P. Single-stranded DNA viruses employ a variety of mechanisms for  
756 integration into host genomes. *Ann N Y Acad Sci*. 2015;1341(1):41–53.
- 757 83. Oren A, Arahal DR, Göker M, Moore ERB, Rossello-Mora R, Sutcliffe IC. International Code of  
758 Nomenclature of Prokaryotes. Prokaryotic Code (2022 Revision). *Int J Syst Evol Microbiol*.  
759 2023;73(5a):005585.
- 760 84. Cumby N, Davidson AR, Maxwell KL. The moron comes of age. *Bacteriophage*. 2012 Oct  
761 1;2(4):e23146.
- 762 85. Martin C, Emerson JB, Roux S, Anantharaman K. A call for caution in the biological interpretation  
763 of viral auxiliary metabolic genes. *Nat Microbiol*. 2025 Aug 27;1–8.
- 764 86. Pratama AA, Bolduc B, Zayed AA, Zhong ZP, Guo J, Vik DR, et al. Expanding standards in  
765 viromics: in silico evaluation of dsDNA viral genome identification, classification, and auxiliary  
766 metabolic gene curation. *PeerJ*. 2021;9:e11447.
- 767 87. Fudyma JD, ter Horst AM, Santos-Medellín C, Sorensen JW, Gogul GG, Hillary LS, et al. Exploring  
768 viral particle, soil, and extraction buffer physicochemical characteristics and their impacts on  
769 extractable viral communities. *Soil Biol Biochem*. 2024;194:109419.

## *Processing Method Shapes Gut Virome Data*

- 770 88. Geonczy SE, Hillary LS, Santos-Medellín, Christian, Sorensen JW, Emerson JB. Patchy burn  
771 severity explains heterogeneous soil viral and prokaryotic responses to fire in a mixed conifer forest.  
772 *mSystems*. 2025 May 14;10(6):e01749-24.
- 773 89. ter Horst AM, Santos-Medellín C, Sorensen JW, Zinke LA, Wilson RM, Johnston ER, et al.  
774 Minnesota peat viromes reveal terrestrial and aquatic niche partitioning for local and global viral  
775 populations. *Microbiome*. 2021 Nov 26;9(1):233.
- 776 90. Andrade-Martínez JS, Camelo Valera LC, Chica Cárdenas LA, Forero-Junco L, López-Leal G,  
777 Moreno-Gallego JL, et al. Computational Tools for the Analysis of Uncultivated Phage Genomes.  
778 *Microbiol Mol Biol Rev*. 2022 Mar 21;86(2):e00004-21.
- 779 91. Olm MR, Crits-Christoph A, Bouma-Gregson K, Firek BA, Morowitz MJ, Banfield JF. inStrain  
780 profiles population microdiversity from metagenomic data and sensitively detects shared microbial  
781 strains. *Nat Biotechnol*. 2021 June;39(6):727–36.
- 782 92. Marine R, McCarren C, Vorrasane V, Nasko D, Crowgey E, Polson SW, et al. Caught in the middle  
783 with multiple displacement amplification: the myth of pooling for avoiding multiple displacement  
784 amplification bias in a metagenome. *Microbiome*. 2014 Jan 30;2(1):3.
- 785 93. Ospino MC, Engel K, Ruiz-Navas S, Binns WJ, Doxey AC, Neufeld JD. Evaluation of multiple  
786 displacement amplification for metagenomic analysis of low biomass samples. *ISME Commun*. 2024  
787 Feb 12;4(1):ycae024.
- 788 94. Roux S, Solonenko NE, Dang VT, Poulos BT, Schwenck SM, Goldsmith DB, et al. Towards  
789 quantitative viromics for both double-stranded and single-stranded DNA viruses. *PeerJ*.  
790 2016;4:e2777.
- 791 95. Yilmaz S, Allgaier M, Hugenholtz P. Multiple displacement amplification compromises quantitative  
792 analysis of metagenomes. *Nat Methods*. 2010 Dec;7(12):943–4.
- 793 96. Jansen D, Matthijnsens J. The Emerging Role of the Gut Virome in Health and Inflammatory Bowel  
794 Disease: Challenges, Covariates and a Viral Imbalance. *Viruses*. 2023 Jan 6;15(1):173.
- 795 97. Chang WS, Harvey E, Mahar JE, Firth C, Shi M, Simon-Loriere E, et al. Improving the reporting of  
796 metagenomic virome-scale data. *Commun Biol*. 2024 Dec 20;7(1):1687.
- 797 98. Castro-Mejía JL, Muhammed MK, Kot W, Neve H, Franz CMAP, Hansen LH, et al. Optimizing  
798 protocols for extraction of bacteriophages prior to metagenomic analyses of phage communities in  
799 the human gut. *Microbiome*. 2015 Nov 17;3(1):1–14.
- 800 99. Haagmans R, Charity OJ, Baker D, Telatin A, Savva GM, Adriaenssens EM, et al. Assessing Bias  
801 and Reproducibility of Viral Metagenomics Methods for the Combined Detection of Faecal RNA and  
802 DNA Viruses. *Viruses*. 2025 Jan 23;17(2):155.

803

804